First-principles evaluation of carbon diffusion in Pd and Pd-based alloys

Chen Ling and David S. Sholl*

School of Chemical and Biomolecular Engineering, Georgia Institute of Technology, Atlanta, Georgia 30332-0100, USA

(Received 12 August 2009; revised manuscript received 28 October 2009; published 3 December 2009)

The absorption and diffusion of carbon in Pd and Pd-based alloys can be important in applications of these materials as catalysts or membranes, but little is known about these processes. We used first principles calculations to characterize the absorption of C in pure Pd and PdM alloys with M=Ag, Au, and Cu. Our calculations show that the preferred configuration of C in Pd is as an interstitial atom; effects from Pd vacancies are minimal and substitutional sites are much less favorable. When the effects of thermal lattice expansion are included, our calculations predict C diffusivities in good agreement with experimental data, which is only available at elevated temperatures. Characterizing the binding energy and hopping energies of interstitial C in terms of lattice expansion or contraction is also a useful way to understand the effect of small amounts of M=Ag, Au, or Cu in PdM alloys. We also examined the properties of interstitial C in $Pd_{77.7}Ag_{22.3}$. Our calculations predict that the diffusivity of C in this alloy is two to three orders of magnitude lower than in pure Pd.

DOI: 10.1103/PhysRevB.80.214202 PACS number(s): 61.72.Bb, 66.30.J−, 61.72.J−

I. INTRODUCTION

Diffusion of carbon in iron group transition metals is important in a number of technologically important processes such as surface hardening and molecule-surface interactions in heterogeneous catalysis.[1,2] For example, due to its relatively high diffusivity, interstitial diffusion of carbon often controls the kinetics of phase transformations and microstructure in steels. The diffusion of carbon in ferrite and austenite has been thoroughly investigated experimentally for over 50 years.[3] However, a description of the atomic details of the diffusion path of carbon in ferrite and austenite from first principle calculations was only given relatively recently.[4]

Pd-based alloys are a well-established material as membranes for separating and purifying hydrogen from mixed gas streams and as a catalyst for hydrogenation reactions.[5,6] One target application for the integration of membrane technologies has been the treatment of syngas streams from gasification processes. The gasification effluent stream typically contains hydrogen mixed with impurities such as carbon dioxide, carbon monoxide, steam, and trace amounts of hydrogen sulfide and ammonia.[7,8] It is clear from both experiments and theoretical calculations that under the conditions where metal membranes would be used, carbon-containing species such as CH_4 and CO can adsorb and react on the metal surface.[9,10] Recent experiments examining heterogeneous catalysis with Pd have indicated that besides surface adsorbed carbon, subsurface carbon also plays an important role in Pd catalyzed alkyne hydrogenation.[1,2] The potential role of dissolved carbon in these applications means that a quantitative understanding of the dissolution and diffusion of carbon in Pd and Pd-based alloys would be useful.

The diffusion of carbon in Pd was studied experimentally by Yokoyama *et al.*,[11] who observed a diffusion activation energy of 1.35 eV for this process. The diffusivity measured for carbon in these experiments was about seven orders of magnitude lower than the diffusivity of hydrogen in Pd at 1223 K.[11] We are not aware of any previous studies that have quantified the diffusion rates of carbon in Pd-based alloys.

In this paper, we report a first principles study of the dissolution and diffusion characteristics of carbon in pure Pd and in PdAg, PdAu, and PdCu alloys. Periodic density-functional theory (DFT) coupled with harmonic transition state theory was used to study the atomic mechanism of solid-state diffusion. Our work is based on first principles methods that have been used in the past to successfully describe the diffusion of hydrogen and oxygen in Ni[12,13] and the diffusion of hydrogen in numerous materials such as Pd based alloys,[14–16] metal sulfides[17,18] and amorphous metals.[19,20] This paper is organized as follows. Section II describes our computational methods, and our calculated results for both pure Pd and Pd-based alloys are presented in Sec. III. Section IV compares our calculated results with the available experimental data for pure Pd. Our conclusions are summarized in Sec. V.

II. METHOD

DFT calculations were performed using the Vienna *ab initio* simulation package (VASP) using the generalized gradient approximation (GGA) with the PW91 functional to describe electron exchange-correlation effects. Ion-electron interactions were described by ultrasoft pseudopotentials. A plane-wave expansion with a cutoff of 300.0 eV is used in all calculations.[21] Geometry relaxations were performed with a conjugate gradient method until the forces on all unconstrained atoms were less than 0.03 eV/Å. A Monkhorst–Pack mesh with $4\times4\times4$ k points was used for all calculations. All of our calculations considered bulk materials, not environments near surfaces, so the supercells in our calculations did not include any interfaces. Previous work by Gracia *et al.* used DFT to examine hopping of subsurface C in Pd(111) surfaces.[22] Preliminary calculations confirmed that spin polarization had no impact on the systems considered here, so calculations were performed without spin polarization.

We studied carbon binding in pure Pd and in selected PdCu, PdAu, and PdAg alloys. Pure Pd has an fcc crystal

structure, and the alloys we considered were assumed to have a substitutionally random fcc structure. This structure is consistent with the experimentally established binary phase diagrams for each alloy we considered.[23] DFT optimization gave a lattice constant 3.960 Å for pure Pd without any interstitial carbon atoms. In all calculations, the volume of the lattice was kept constant and all atoms were free to move during the calculation, as appropriate for examining an interstitial species with a low concentration. In a supercell containing 27 Pd atoms, an interstitial carbon in an octahedral site distorted the Pd atoms in the nearest neighbor shell by 0.048 Å. This number decreased to 0.018 and 0.001 Å for Pd atoms in the next nearest and third nearest shell, respectively. After performing a series of calculations with supercells containing 4, 16, 27, 32, and 64 Pd atoms, we found that when the supercell size was increased beyond 27 Pd atoms, the calculated binding energy of carbon changed by less than 0.02 eV relative to the result from the supercell with 27 Pd atoms. As a result, all our subsequent calculations for bulk materials were performed using a supercell containing 27 metal atoms.

Transition states for diffusion of carbon were determined using the nudged elastic band (NEB) method.[24] The vibrational frequencies of local minima and transition states were calculated in the harmonic approximation by assuming that localized vibrations of carbon atoms are decoupled from vibrations of the metal atoms. This procedure gives three real frequencies at a local energy minimum and two real frequencies and one imaginary frequency at a transition state.

III. RESULTS

A. Adsorption and diffusion of carbon in pure Pd

Previous reports indicate that light elements including H, N, C, and O typically occupy the interstitial site rather than substitute the lattice atoms of metals.[4,20] To establish whether this is also the case for C in Pd, we calculated the binding energies of interstitial and substitutional C. The binding energy of interstitial carbon was calculated as

$$E_b = E_{MC} - E_M - E_C. \tag{1}$$

Here, E_b, E_{MC}, E_M, and E_C are the binding energy, the total energy of the metal in the presence of interstitial carbon, the total energy of the pure metal, and the reference carbon energy, respectively. The reference state of carbon is chosen to be gaseous CH_4, one potential source of carbon in the process of purifying hydrogen. With this choice, E_C is defined by

$$E_C = E_{CH_4} - 2E_{H_2}. \tag{2}$$

Here, E_{CH_4} and E_{H_2} are the zero point energy corrected total energies of gaseous CH_4 and H_2, correspondingly. Zero point energies were calculated within the harmonic approximation.

Two kinds of interstitial sites exist in the fcc lattice of pure Pd, the octahedral site (O site) and the tetrahedral site (T site). Figure 1 shows the calculated binding energies for possible configurations of interstitial carbon in pure Pd with the DFT-optimized lattice constant of 3.960 Å. The binding

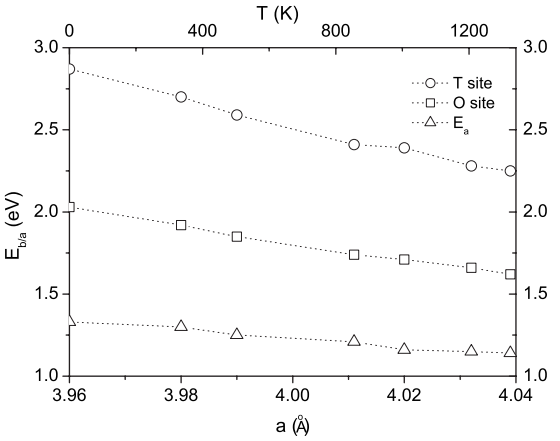

FIG. 1. The binding energies and diffusion barriers of interstitial carbon in pure Pd as a function of lattice constants or temperature calculated as described in the text.

energy of interstitial carbon in the O site is 2.03 eV, which indicates the interstitial carbon configuration is unfavorable compared to gaseous CH_4. Interstitial C in the O site, however, is more stable than the interstitial species in the T site by ~0.8 eV.

We estimated the substitutional energy of a C atom by calculating

$$E_s = E_{M_{n-1}C} - \frac{n-1}{n}E_M - E_C. \tag{3}$$

Here, n is the number of Pd atoms in the defect-free supercell, which is 27 in our calculations, and $E_{M_{n-1}C}$ is the total energy of a supercell with $n-1$ metal atoms and a single substitutional carbon atom. We found the substitutional energy to be 6.2 eV, which is much higher than the interstitial configurations. This indicates that the substitutional configuration is highly unfavorable. As a result, we only consider interstitial carbon in our following calculations.

Metal vacancies have been found to play an important role in absorption of C in metastable Fe-C alloys.[25] Since the presence of H is known in some circumstances to increase the vacancy concentration in Pd,[26] we examined the interaction between C and vacancy defects in Pd. Specifically, we calculated the binding energies of carbon with a Pd vacancy in the nearest-neighbor shell of the interstitial sites. The interaction energy between interstitial C and a Pd vacancy, E_I, was defined by

$$E_I = E_{VC} - \frac{n-1}{n}E_M - E_b - E_C, \tag{4}$$

where E_{VC} is the total energy of the supercell containing the interstitial carbon-vacancy cluster. With this definition, a positive interaction energy is found when an interstitial-vacancy pair is favored compared to having both defects isolated in the crystal. The calculated interaction energy was 0.13 eV for the O site and 0.11 eV for the T site. Although interstitial C is slightly stabilized by these vacancies, the large formation energy for Pd vacancies suggests that interstitial-vacancy complexes will play a relatively minor

role in the absorption of C in Pd, unlike the situation in Fe-C systems.[25]

We now turn to describing the diffusion of interstitial C in Pd. Because the O site is the most stable location for interstitial C, we considered processes that allowed C to hop from an O site to another nearest neighbor O site. Two possible hopping paths were chosen in NEB calculations. The first one starts from an O site, passes through a T site and ends at another O site,[12,16] while the second one connects two O sites directly.[4,13] The former path is typically expected to be the dominant diffusion path in fcc metals, but the latter path has been reported for C diffusion in austenite at low concentration,[4] and O hopping in Ni.[13] We found, however, that C cannot diffuse in Pd via the latter path at any appreciable rate. That is, the only physically relevant hopping path starts in an O site and passes through a T site before ending at another O site. The converged minimum energy path for this process is symmetric, with a double maxima and one intermediate local minimum at the T site. The energy barrier between the O site and the transition state is 1.33 eV using the DFT-optimized lattice constant. Hopping from a T site to an O site proceeds with a barrier of 0.49 eV, so this is a much faster process than O to T hopping.

As the existence of a Pd vacancy slightly favors the interstitial carbon, we also studied how vacancies affect the diffusion of carbon by calculating the hopping barriers in the vicinity of a Pd vacancy. Several possible configurations of O sites were checked for both the initial and final state in NEB calculations. The lowest barrier was found to be the hopping with a Pd vacancy in the nearest-neighbor (NN) shell of the interstitial carbon at O sites for both initial and final state, followed by the hop with a Pd vacancy in the nearest and next-nearest-neighbor (NNN) shell of the interstitial carbon for the initial state and the final state, respectively. Even for the lowest barrier, the existence of a Pd vacancy decreases the barrier by less than 0.1 eV. This observation further supports the idea that Pd vacancies do not play an important role in the absorption and diffusion of carbon in Pd. We did not consider the contribution of metal vacancies in the remainder of our calculations.

All of the results described above were based on calculations performed with the DFT-optimized lattice parameter for Pd, 3.960 Å. For interstitial species that are mainly relevant at high temperatures, it is useful to consider whether the characteristics of interstitial diffusion are affected by thermal expansion of the metal.[12,13] Figure 1 shows the DFT-calculated binding energies and diffusion activation energies of C in Pd for several different lattice constants in the range of 3.96–4.04 Å. Each quantity listed in the table decreases approximately linearly with the lattice constant over this range. As the lattice constant changes from 3.96 to 4.04 Å, the O site binding energy decreases by 0.41 eV, while the activation energy to hop out of an O site decreases by 0.19 eV.

To connect the data above with the effects of thermal expansion on C diffusion in Pd, we must define the temperature-dependent lattice constant of Pd. Two equations describing the experimentally observed lattice thermal expansion of Pd have been reported. The first one was given by Dutta *et al.*,[27] where the lattice constant (in m) is given as

$$a_T = 3.889 \times 10^{-10} + 4.5 \times 10^{-15} T + 1.37 \times 10^{-18} T^2. \quad (5)$$

The second equation was reported by Lu *et al.*[28] who characterized the molar volume of Pd as

$$V_T = V_0 e^{3.11002 \times 10^{-5} T + 7.4407 \times 10^{-9} T^2}. \quad (6)$$

Here, V_T (V_0) is the molar volume at temperature T (0 K). These two equations define lattice constants that differ by less than 0.15 Å for $T < 1400$ K. We cannot use these lattice constants directly in interpreting our DFT calculations because of the small difference that exists between the DFT-optimized lattice constant at 0 K and the experimental observation. We therefore predicted the relevant lattice constant to use in applying our DFT data by multiplying the ratio a_T/a_0 measured in experiments with the DFT-optimized lattice constant. At each temperature, we used the average of Eqs. (5) and (6) as the experimental value. Using the above assumptions, we show how the binding energies and activation energy barriers for C diffusion in Pd change with temperature in Fig. 1. Changing the temperature from 0 to 1000 K is seen to reduce the binding energy of C in an O site by ~0.25 eV and the diffusion activation energy by ~0.1 eV.

B. Adsorption and diffusion of carbon in Pd-based alloys

One key application of Pd based membranes is to purify hydrogen from gas mixtures. Because pure Pd membranes are prone to hydrogen embrittlement and poisoning by *S*-containing species, Pd-based alloys are useful materials for these applications.[18] PdAg alloys have been widely considered because they can show an improved permeability of hydrogen compared with pure Pd.[29,30] PdCu alloys have been reported to be more resistant to sulfur poisoning than pure Pd.[15] We know of no previous studies that have quantified the solubility or diffusivity of C in Pd-based alloys such as these. To provide some initial information on this topic, we extended our calculations to examine interstitial C in $Pd_{96}M_4$ alloys with M=Ag, Cu and Au to see how a low concentration of the non-Pd metal affects interstitial C. We then turned to a more complicated alloy, $Pd_{77.7}Ag_{22.3}$, to show how carbon behaves in an alloy that is already used in the practical applications.[3] In every case, we have defined the alloy composition in at.%. All of these alloys are known to be substitutionally random fcc crystals at elevated temperatures.[23] For each alloy, all calculations were performed using a 27 atom supercell with a DFT-optimized lattice constant. The lattice constant for each alloy is listed in Table I. Compared to pure Pd, the presence of Cu decreases the alloy lattice constant while Ag or Au increases the lattice constant.

Similar to what we did for pure Pd, we calculated the binding energies of interstitial C in both O and T sites. In substitutionally random $Pd_{96}M_4$ alloys, more than 99% of O sites can be divided into three categories if the sites are characterized simply by the atoms forming the nearest neighbor (NN) and next nearest neighbor (NNN) shells of atoms around the site.[16] These sites have one M atom in the NN shell but pure Pd in the NNN shell (denoted NN-O), one M atom in the NNN shell but no M atoms in the NN shell (denoted NNN-O), or no M atoms in the NN or NNN shells

TABLE I. The binding energies and diffusion barriers for O to T hops of interstitial carbon in $Pd_{96}Cu_4$, $Pd_{96}Au_4$, $Pd_{96}Ag_4$, and $Pd_{77.7}Ag_{22.3}$.

Composition	$Pd_{96}Cu_4$		$Pd_{96}Au_4$		$Pd_{96}Ag_4$		$Pd_{77.7}Ag_{22.3}$
Lattice constant (Å)	3.953		3.968		3.970		4.011
E_b (eV)	NO-O	2.12	NO-O	1.97	NO-O	1.92	O 1.70–3.03
	NNN-O	2.08	NNN-O	1.98	NNN-O	1.93	
	NN-O	2.21	NN-O	2.29	NN-O	2.18	
	NO-T	2.97	NO-T	2.79	NO-T	2.80	T 2.42–4.05
E_a (eV)	1.36		1.31		1.30		1.20–1.25

(denoted NO-O). We similarly defined NN-T, NNN-T and NO-T sites. In each alloy, the NN-O site has the least favored binding energy among the O sites we examined, indicating that interstitial C will not typically be found in these sites. In $Pd_{96}Ag_4$ and $Pd_{96}Cu_4$, the NNN-O site has the lowest binding energies, while in $Pd_{96}Au_4$ the NO-O and NNN-O site have very similar binding energies. Similar to the effect caused by the thermal expansion of pure Pd, the binding energies at NO-O sites become more favorable as the lattice constant of the alloy is increased. For T sites, we found that including an M atom in the NN or NNN shell increases the binding energy by about 0.3 eV. The NO-T sites are the most stable T site in all three alloys.

To study the diffusivity of carbon in $Pd_{96}M_4$ alloys, we chose the hop beginning with a NO-O site, passing through a NO-T site, and ending at a NO-O site, as these two O sites were the most stable configurations in each alloy. The activation energy barriers from a NO-O site to the transition state in these three alloys are listed in Table I. The barrier from a NO-T site to the transition state can be defined by the difference of the binding energies at NO-O site and NO-T site. Although this barrier decreases with the lattice constant, the decreasing trend is less significant than the binding energies. The difference between the highest barrier, in $Pd_{96}Cu4$, and the lowest barrier, in $Pd_{96}Ag_4$, is only 0.05 eV, while this value is 0.2 eV for the binding energies.

We now turn to $Pd_{77.7}Ag_{22.3}$. One key difference between $Pd_{77.7}Ag_{22.3}$ and $Pd_{96}M_4$ is that a much larger number of local configurations can exist for the interstitial sites in the former material than in the latter. Instead of attempting to describe every possible site in $Pd_{77.7}Ag_{22.3}$ with DFT, we examine the set of 27 O sites in a single computational supercell containing 21 Pd atoms and 6 Ag atoms that were randomly distributed on the lattice sites in the supercell. Previous studies of interstitial H in PdM alloys revealed that the binding energies of interstitial H are correlated with the number of Pd atoms in the nearest and next nearest shell.[14] We found a similar behavior for interstitial C in $Pd_{77.7}Ag_{22.3}$. Figure 2 shows the calculated O site binding energies as a function of the number of Pd atoms in the NN shell. The scatter of the results in Fig. 2 shows that using the number of Ag atoms in the NN shell alone cannot fully describe the binding energies in this alloy, as expected.[16] Nevertheless, simply counting the number of Ag atoms in this shell captures much of the variation in the observed binding energies; O sites without any Ag atoms in the NN shell have the lowest binding energies and the binding energies increases by ~0.25 eV/Ag atom as the number of Ag atoms in the NN shell is increased. This variation is a direct indication of the fact that it is not just the lattice constant that determines the binding energy of a particular interstitial site; the chemical identity of the atoms near the site is also important. This trend is consistent with our observation from $Pd_{96}Ag_4$ that interstitial C is more unfavorable in the NN sites than in the NO site. Although increasing the Ag content from $Pd_{96}Ag_4$ to $Pd_{77.7}Ag_{22.3}$ creates more sites that are unfavorable for interstitial C because of the presence of nearby Ag atoms, the binding energy of the most favorable sites in the Ag-rich alloy is significantly lower than in the Ag-poor alloy. The most favorable site we observed in the $Pd_{77.7}Ag_{22.3}$ alloy has a binding energy ~0.3 eV lower than the O sites in pure Pd, an effect that can be attributed to the expanded lattice constant of the alloy relative to pure Pd. The fact that a significant fraction of the O sites in the $Pd_{77.7}Ag_{22.3}$ alloy have lower binding energies for C than the O sites in pure Pd indicates that at equilibrium the concentration of interstitial C in the alloy will be higher than in the pure metal.

To estimate how increasing the Ag content of the alloy changes the hopping of C between interstitial sites, we characterized the eight distinct hops that can occur from the O site with the lowest binding energy observed in $Pd_{77.7}Ag_{22.3}$. The calculated activation energies for this process, as shown in Table I, were 0.08–0.13 eV lower than the value in pure Pd. We performed similar calculations for another O site in the alloy with one Ag atom in the NN shell whose binding energy is 0.31 eV higher than the lowest one. In this case

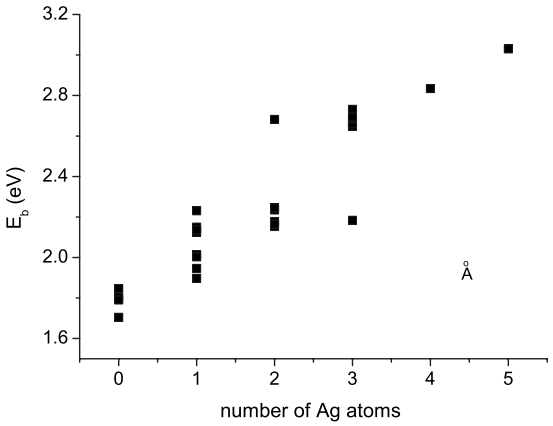

FIG. 2. The binding energies of interstitial carbon in O sites of $Pd_{77.7}Ag_{22.3}$ as a function of the number of Ag atoms in the nearest neighbor shell.

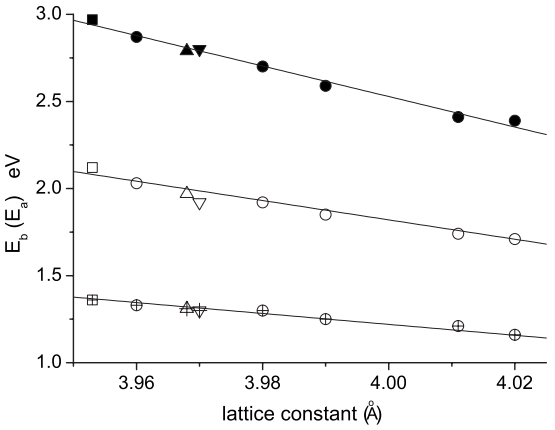

FIG. 3. The binding energy and O to T activation energy as a function of the lattice constant in pure Pd and $Pd_{96}M_4$ alloys with M=Cu, Au, and Ag. Solid symbols: T sites, open symbols: O sites, symbols with crosses: activation energy. Circle: pure Pd, square: $Pd_{96}Cu_4$, upward pointing triangle: $Pd_{96}Au_4$, downward pointing triangle $Pd_{96}Ag_4$. Lines: fitting value from Eq. (6).

both the initial configuration and the final configurations were different from the previous set of calculations. The hopping barriers, however, were found to be 1.22–1.26 eV. That is, all of the activation barriers for hopping out of these two distinct O sites were found to lie within a narrow range of energy.

IV. DISCUSSION

Above, we examined the absorption and diffusion of behavior of C in both pure Pd and Pd based alloys. In both pure Pd and Pd-based alloys, increasing the lattice constant favors both the stability and hopping of interstitial carbon atoms. Further examination shows that despite the possible different environments outside of the nearest neighbor shell of the interstitial carbon atoms, we can use the same equations to describe the binding energies and the activation energy barriers of interstitial carbon in a NO-type site in both Pd and Pd-based alloys, as shown in Fig. 3. The equations are fitted to describe the linear decreasing trend of the binding energies of the NO-type sites and hopping barriers with energy in eV as shown below:

$$E_{b,O} = -5.55a + 24.02,$$

$$E_{b,T} = -8.75a + 37.53,$$

$$E_a = -3.13a + 13.74. \tag{7}$$

Here $E_{b,o}$, $E_{b,T}$, and E_a are the binding energy at the O sites, T sites, and the activation energy barrier, and a is the lattice constant of the metal (in Å).

For $Pd_{77.7}Ag_{22.3}$, as we have discussed above, the binding energies in the interstitial sites depend strongly on the number of Ag atoms in the nearest-neighbor shell, but the hopping barriers out of an O site, however, are roughly independent of the environment. These characteristics can be described using (in eV)

$$E_{b,O} = 1.75 + 0.253n_{Ag},$$

$$E_{b,T} = 2.57 + 0.240n_{Ag},$$

$$E_a = 1.25. \tag{8}$$

Here n_{Ag} is the number of Ag atoms in the nearest-neighbor shell of the relevant interstitial site.

Once we have calculated the adsorption energy of interstitial carbon and activation barriers of the hopping in pure Pd, the diffusivity of the interstitial carbon can then be estimated by considering hopping between interstitial sites. The net diffusivity can be written as[31]

$$D = n\beta d^2/\bar{t}, \tag{9}$$

where n is the number of nearest-neighbor sites for a diffusing interstitial atom, β=0.25 is the probability that a jump from an O to a T site and a subsequent jump from the T site to an independently chosen O site advances the particle along a particular direction of diffusion, and d is the length of the jump projected onto the direction of diffusion, which is $0.5a$ in fcc metals where a is the lattice constant. k is the average time required for one hop, which is

$$\bar{t} = \frac{1}{k_{O-T}} + \frac{1}{k_{T-O}}. \tag{10}$$

Here, k_{O-T} (k_{T-O}) is the hopping rate from O site to T site (T site to O site). We calculated the site to site hopping rates using the quantum corrected harmonic transition state theory as[14]

$$k_{O-T} = \frac{\prod_{i=1}^{3} \upsilon_o f(h\upsilon_i/2kT)}{\prod_{j=1}^{2} \upsilon_j^{TS} f(h\upsilon_j^{TS}/2kT)} e^{-E_{a,OT}/k_bT}$$

$$k_{T-O} = \frac{\prod_{i=1}^{3} \upsilon_T f(h\upsilon_i/2kT)}{\prod_{j=1}^{2} \upsilon_j^{TS} f(h\upsilon_j^{TS}/2kT)} e^{-E_{a,TO}/k_bT}. \tag{11}$$

Here ν_o, ν_T, and ν_j^{TS} are the vibrational frequencies at the O site, T site and transition state, respectively, k_b and h are Boltzmann's constant and Planck's constant, $f(x)=\sinh(x)/x$ and $E_{a,OT}$ ($E_{a,TO}$) is the barrier for a hopping from O site to T site (T site to O site). As $E_{a,TO}$ is much lower than $E_{a,OT}$, $k_{T-O} \gg k_{O-T}$ and we can simplify Eq. (10) to

$$\bar{t} = \frac{1}{k_{O-T}}. \tag{12}$$

Figure 4 shows the calculated diffusivity of carbon in pure Pd with and without the effects of thermal expansion on the lattice constant. When thermal expansion was included, the T-dependent lattice constant was estimated as described previously and the diffusion activation energies were defined using Eq. (7). To apply Eq. (11) in our calculations, we calculated the zero point energies (ZPEs) of C in an O site, T

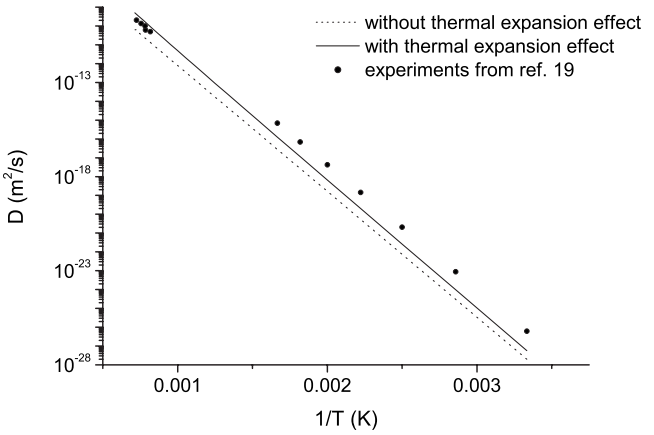

FIG. 4. Predicted and experimentally observed diffusivity of C in pure Pd. The experimental measurements came from the report of Yokoyama *et al.* (Ref. 11). The calculated value showed both the result with and without considering thermal expansion of the lattice, as described in the text.

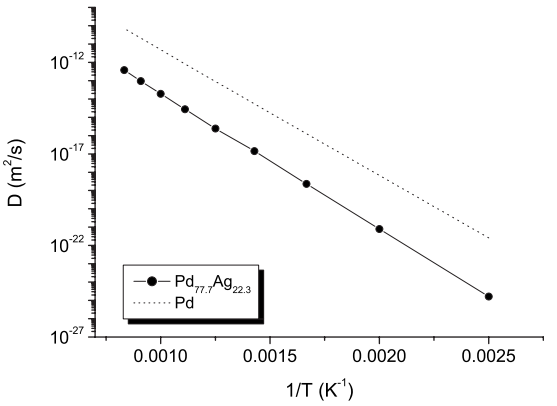

FIG. 5. Predicted diffusivity of C in $Pd_{77.7}Ag_{22.3}$ and in pure Pd

site and transition state with different lattice constants. Unlike the binding energies, we found that the ZPE is almost independent of lattice constant. For example, when the lattice constant changes from 3.96 to 4.02 Å, the ZPE in the O site only decreases by 0.008 eV. Thus, we use the vibrational frequencies from Pd with the DFT-optimized lattice constant at all temperatures. In order to compare the estimated diffusivity with experimentally measured values, the available experimental data is also shown in Fig. 4. The experimental data gives an activation energy of 1.37 eV at high temperature (1223–1378 K) and 1.32 eV at low temperature (300–640 K).[11] When we do not consider thermal expansion effects, we predict a net activation energy of 1.33 eV (1.35 eV) in the same high (low) temperature ranges and the diffusivity is ~4 (20) times lower than the high (low) temperature experimental values. After including thermal expansion effects, our calculations give a net activation energy of 1.25 eV (1.30 eV) in the high (low) temperature ranges. The diffusivity predicted with this approach is ~1.5 higher than the experimental value at high temperatures and ~8 times lower than the low-temperature experimental values. When the small apparent inconsistency between the experimentally observed diffusivities at high and low temperatures are considered, we conclude that our first principles calculations accurately describe the diffusion of interstitial C in Pd.

Due to the structure complexity of $Pd_{77.7}Ag_{22.3}$ alloys, an accurate calculation of the diffusivity of C in this material must consider all possible hopping paths in this alloy. Semidey-Flecha and Sholl have used methods based on cluster expansions to approach this task for H diffusion in metal alloys.[16] This approach is feasible when DFT data for a large collection of interstitial sites and transition states are available. Because we only generated DFT data for a limited number of transition states, we adopted a more approximate approach for estimating the diffusivity of C in $Pd_{77.7}Ag_{22.3}$. In these calculations, we generated a large substitutionally random simulation volume, then assigned the interstitial site and transition state binding energies using Eq. (8). We also assumed that the vibrational frequencies at different interstitial sites and transition states were independent of their the surrounding environment. The same kinetic Monte Carlo methods used by Semidey-Flecha and Sholl[16] were then used to compute the diffusivity within this model. Figure 5 shows the diffusivity calculated in this way for $Pd_{77.7}Ag_{22.3}$ as well as the previous results for pure Pd that included thermal expansion effects. The results for the PdAg alloy did not include effects from thermal expansion. From 600–1200 K, the predicted diffusivity in $Pd_{77.7}Ag_{22.3}$ is two to three orders of magnitude lower than in pure Pd. It is interesting to note that for H diffusion in the same system, the diffusivity only decreases about 25% when the Ag content increases from 0 to 20%.[29] To explain this difference, we calculated the binding energies of H in PdAg alloys. These calculations show that adding a Ag atom in the nearest neighbor shell of an interstitial site only increases the binding energy by about 0.05 eV, while this value is 0.25 eV for carbon. This indicates, as might be expected, that the potential energy surface for interstitial C is affected more strongly by the presence of Ag in the alloy than for interstitial H.

The effective activation energy barrier for C diffusion in $Pd_{77.7}Ag_{22.3}$ obtained from Fig. 5 is 1.47 eV. The difference between this value and the value for the local hops described in Table I is close to the energy change associated with adding one Ag atom in the nearest neighbor shell of an O site. This similarity is not a coincidence; it indicates that in the PdAg alloy, long-range diffusion of carbon must involve processes that move C from interstitial sites into neighboring interstitial sites that have an additional Ag atom in their NN shell. Even though the hopping barriers out of the distinct O sites we examined in Table I lay in a narrow range, the new barrier to hop from an O site into an adjacent T site and then onto a new O site will be dominated by the higher of the two intermediate barriers along this local path.

V. SUMMARY

We performed periodic DFT calculations of the absorption and diffusion of carbon in pure Pd and the Pd based alloys PdM with M=Cu, Ag, and Au. In pure Pd, the most stable location for carbon is as an interstitial atom in an octahedral site. The binding energy in this site is endo-

thermic by 2.03 eV compared with carbon in gaseous CH_4. Substitutional C is even less stable, and our calculations indicate that Pd vacancies will play at most a minor role in the population of interstitial C. The minimum energy path for carbon diffusion starts from an octahedral site, passes through an adjacent tetrahedral site and ends at another octahedral site. At low temperatures where thermal expansion of the metal can be neglected, our calculations have a diffusion barrier of 1.33 eV.

We found that in both Pd and Pd-based alloys, the endothermic binding energy of C and the activation energy for interstitial diffusion decrease as the host's lattice parameter increases. Because the available experimental data for C diffusion in Pd is at elevated temperatures, it was important to include the effects of thermal lattice expansion when assessing the diffusivity of C in Pd. At temperatures above 1000 K, the diffusivity predicted via transition state theory is roughly an order of magnitude larger once thermal expansion effects are included than when the low temperature lattice constant for Pd was used. The diffusivity predicted by our calculations was in good agreement with the available experimental data.

In PdM alloys with low concentrations of M=Ag, Au, or Cu, the binding energy of interstitial C at sites with no M atoms in the nearest neighbor shell could be understood from the lattice expansion or contraction in the alloy relative to pure Pd. In each of these alloys, the binding energy of interstitial carbon increases with the number of M atom in the nearest neighbor shell. Of the three alloys we considered, PdCu has the smallest lattice constant, thus it has the least favorable binding energies for interstitial C and the highest diffusion barriers. We also examine the properties of interstitial C in a more complex PdAg alloy, $Pd_{77.7}Ag_{22.3}$. By examining the binding energies and local activation energy for site to site hops in a range of sites in this alloy, we estimated the net diffusivity of C. Our calculations predict that C diffusion in this alloy is 2–3 orders of magnitude slower than in pure Pd.

ACKNOWLEDGMENT

This work was supported by a grant from the U.S. DOE Hydrogen Fuels Initiative.

*Corresponding author; david.sholl@chbe.gatech.edu

[1] D. Teschner, J. Borsodi, A. Wootsch, Z. Revay, M. Havecker, A. Knop-Gericke, S. D. Jackson, and R. Schlogl, Science **320**, 86 (2008).
[2] D. Teschner, E. Vass, M. Havecker, S. Zafeiratos, P. Schnorch, H. Sauer, A. Knop-Gericke, R. Schlogl, M. Chamam, A. Wootsch, A. S. Canning, J. J. Gamman, S. D. Jackson, J. MacGregor, and L. F. Gladden, J. Catal. **242**, 26 (2006).
[3] S. Uemiya, T. Matsuda, and E. Kikuchi, J. Membr. Sci. **56**, 315 (1991).
[4] D. E. Jiang and E. A. Carter, Phys. Rev. B **67**, 214103 (2003).
[5] W. Liu, B. Q. Zhang, and X. F. Liu, Prog. Chem **18**, 1468 (2006).
[6] D. S. Sholl and Y. H. Ma, MRS Bull. **31**, 770 (2006).
[7] H. Gao, Y. S. Lin, Y. Li, and B. Zhang, Ind. Eng. Chem. Res. **43**, 6920 (2004).
[8] M. Mundschau and X. Xie, Catal. Today **118**, 12 (2006).
[9] Y. Ma, J. Bansmann, T. Diemant, and R. J. Behm, Surf. Sci. **603**, 1046 (2009).
[10] K. M. Neyman, C. Innatam, A. B. Gordienko, I. V. Yudanov, and N. Rosch, J. Chem. Phys. **122**, 174705 (2005).
[11] H. Yokoyama, H. Numakura, and M. Koiwa, Acta Mater. **46**, 2823 (1998).
[12] E. Wimmer, W. Wolf, J. Sticht, P. Saxe, C. B. Geller, R. Najafabadi, and G. A. Young, Phys. Rev. B **77**, 134305 (2008).
[13] E. H. Megchiche, M. Amarouche, and C. Mijoule, J. Phys.: Condens. Matter **19**, 296201 (2007).
[14] P. Kamakoti and D. S. Sholl, Phys. Rev. B **71**, 014301 (2005).
[15] P. Kamakoti, B. D. Morreale, M. V. Ciocco, B. H. Howard, R. P. Killmeyer, A. V. Cugini, and D. S. Sholl, Science **307**, 569 (2005).
[16] L. Semidey-Flecha and D. S. Sholl, J. Chem. Phys. **128**, 144701 (2008).
[17] C. Ling and D. S. Sholl, J. Membr. Sci. **329**, 153 (2009).
[18] B. D. Morreale, B. H. Howard, O. Iyoha, B. M. Enick, C. Ling, and D. S. Sholl, Ind. Eng. Chem. Res. **46**, 6313 (2007).
[19] S. Q. Hao and D. S. Sholl, J. Chem. Phys. **130**, 244705 (2009).
[20] S. Q. Hao, M. Widom, and D. S. Sholl, J. Phys.: Condens. Matter **21**, 115402 (2009).
[21] G. Kresse and J. Hafner, Phys. Rev. B **48**, 13115 (1993).
[22] L. Gracia, M. Calatayud, J. Andrés, C. Minot, and M. Salmeron, Phys. Rev. B **71**, 033407 (2005).
[23] T. B. Massalski, H. Okamoto, P. R. Subramanian, and L. Kacprzak, *Binary Alloy Phase Diagrams* (ASM International, Materials Park, Ohio, 1990), p. 3.
[24] G. Henkelman, B. P. Uberuaga, and H. Jonsson, J. Chem. Phys. **113**, 9901 (2000).
[25] C. J. Forst, J. Slycke, K. J. Van Vliet, and S. Yip, Phys. Rev. Lett. **96**, 175501 (2006).
[26] Y. Fukai and N. Okuma, Phys. Rev. Lett. **73**, 1640 (1994).
[27] B. N. Dutta and B. Dayal, Phys. Status Solidi B **3**, 2253 (2006).
[28] X. G. Lu, M. Selleby, and B. Sundman, CALPHAD: Comput. Coupling Phase Diagrams Thermochem. **29**, 68 (2005).
[29] G. L. Holleck, J. Phys. Chem. **74**, 503 (1970).
[30] C. G. Sonwane, J. Wilcox, and Y. H. Ma, J. Phys. Chem. B **110**, 24549 (2006).
[31] C. Wert and C. Zener, Phys. Rev. **76**, 1169 (1949).